13892 CALIBRATION FOR 1-D UNSTEADY FLOW MODELS

KEY WORDS: **Calibration;** Channels; Coefficients; Computers; Fluid flow; **Friction coefficient (hydraulic);** Hydraulics; Identification; Manning formula; Mathematical models; **Open channel flow;** Optimization; Parameters; **Rivers; Unsteady flow;** Water flow

ABSTRACT: This paper presents a simple and efficient optimization technique for determining the continuous piecewise linear variation of the roughness parameter with discharge (or stage) for each reach of the river system bounded by gaging stations or major tributary confluences. The optimization technique is based on a modified Newton-Raphson gradient-type algorithm and the application of a decomposition principle that simplifies the treatment of complex river systems of dendritic (tree-type) configuration. The observed-computed stage hydrograph RMS errors coincident with the optimal roughness-discharge relationship range from essentially zero for ideal systems with no observational errors from 0.2 ft to 0.7 ft (0.06 to 0.21 m) for complex natural systems. The required computation time (IBM 360-195) is about 0.005 sec per time step per distance step when the optimization technique is coupled with a weighted four-point implicit finite difference approximation of the unsteady flow equations.

JOURNAL OF THE HYDRAULICS DIVISION

CALIBRATION TECHNIQUE FOR 1-D UNSTEADY FLOW MODELS

By Danny L. Fread,[1] M. ASCE and George F. Smith,[2] A. M. ASCE

INTRODUCTION

An essential step in the application of the unsteady flow equations to flood routing and streamflow modeling activities is the determination of the roughness parameter in the friction slope term of the momentum equation. The one-dimensional equations of unsteady flow in a nonprismatic channel consist of a continuity equation and a momentum equation, i.e.

$$\frac{\partial Q}{\partial x} + \frac{\partial (A + A_o)}{\partial t} - q = 0 \quad \ldots\ldots\ldots\ldots\ldots\ldots\ldots\ldots\ldots\ldots (1)$$

$$\frac{\partial Q}{\partial t} + \frac{\partial \frac{Q^2}{A}}{\partial x} + gA\left(\frac{\partial h}{\partial x} + S_f\right) - qv_x = 0 \quad \ldots\ldots\ldots\ldots\ldots\ldots\ldots\ldots (2)$$

in which $$S_f = \frac{n^2 Q|Q|}{2.21 A^2 R^{4/3}} = \frac{Q|Q|}{C^2 A^2 R} \quad \ldots\ldots\ldots\ldots\ldots\ldots\ldots\ldots (3)$$

and $h(x,t)$ = water surface elevation; x,t = space and time variables; $A(x,h)$ = active cross-sectional area of water; $A_o(x,h)$ = inactive (off-channel storage) cross-sectional area of water; $Q(x,t)$ = discharge; $q(x,t)$ = lateral inflow or outflow per unit length of channel; $v_x(x,t)$ = velocity of lateral inflow in direction of channel flow; g = acceleration due to gravity; S_f = friction slope; R = hydraulic radius; n = Manning roughness coefficient; and C = Chezy resistance coefficient.

In modeling one-dimensional unsteady flows, Eqs. 1 and 2 are applied for

Note.—Discussion open until December 1, 1978. To extend the closing date one month, a written request must be filed with the Editor of Technical Publications, ASCE. This paper is part of the copyrighted Journal of the Hydraulics Division, Proceedings of the American Society of Civil Engineers, Vol. 104, No. HY7, July, 1978. Manuscript was submitted for review for possible publication on October 17, 1977.

[1]Research Hydro., Hydrologic Research Lab., Office of Hydrology, National Weather Service, NOAA, Silver Spring, Md.

[2]Research Hydro., Hydrologic Research Lab., Office of Hydrology, National Weather Service, NOAA, Silver Spring, Md.

previously observed unsteady flow events. The optimum n functions are determined such that the absolute value of the sum of the differences between the observed and computed stages or discharges is minimized. The computed values are determined from a finite difference solution of the unsteady flow equations, Eqs. 1 and 2, subject to the initial and boundary conditions of Eqs. 4–9. Although the technique is not restricted to the particular finite difference method used to solve the unsteady flow equations, it was developed to be conveniently and inexpensively used with implicit finite difference techniques applied to dendritic (tree-type) river systems. It is equally applicable to explicit finite difference solution techniques applied either to a single river or to a river system. The technique is applied to an ideal channel, a main-stem river, and a natural dendritic river system to demonstrate its accuracy and economy.

Relation to Previous Research

The determination of parameters in a set of partial differential equations subject to specified boundary and initial conditions is known in the literature as the inverse problem. Much of the previous work in solving the inverse problem for hydraulic systems has been concentrated in the solution of two-dimensional unsteady ground-water equations for aquifers. Solution techniques for the aquifer parameter identification problem have included: (1) Quasilinearization used by Yeh and Tauxe (18,19), Marino and Yeh (14), and Lin and Yeh (13); (2) linear programming used by Kleinecke (12); (3) multiple-objective linear programming used by Neuman (15); (4) a Galerkin finite element approach for steady-state input used by Frind and Pinder (9); and (5) Marquardt's nonlinear estimation algorithm used by Garay, Haines, and Das (10). For one-dimensional unsteady open-channel flow models, parameter identification methods have included: (1) The influence coefficient method used by Becker and Yeh (2,3) and Bennett (4); (2) linear programming used by Yeh and Becker (17); and (3) the conjugate gradient method used by Rao, Contractor, and Tiyamani (16).

The previous studies in parameter identification, both for aquifer and open-channel models, have used the minimization of the root-mean-square error as a criterion in determining optimal parameters. The technique presented in this paper minimizes the bias (absolute value of the sum of the differences between observed and computed stages or discharges) to determine the optimal value. The bias was selected since it lent itself to a very simple mathematical technique and has proven to eliminate most of the error of the root-mean-square. This is demonstrated in the applications presented herein.

Much of the previous work in parameter identification has dealt with constant parameter(s), whereas in this paper, a single parameter that varies with space

the purpose of determining the unknowns, h and Q, as functions of x and t. Of course, the solution is subject to boundary conditions at the upstream and downstream extremities of the subcritical unsteady flow reach, lateral inflow throughout the reach, and initial conditions of h and Q along the reach at $t = 0$. Typical boundary and initial conditions are

$$Q_1(t) = Q'(t) \quad \ldots \quad (4)$$

$$h_N(t) = h'(t) \quad \ldots \quad (5)$$

$$h(x,0) = h_o(x) \quad \ldots \quad (6)$$

$$Q(x,0) = Q_o(x) \quad \ldots \quad (7)$$

$$q(x,t) = q'(x,t) \quad \ldots \quad (8)$$

$$v_x(x,t) = v'_x(x,t) \quad \ldots \quad (9)$$

in which $Q'(t)$, $h'(t)$, $q'(x,t)$, and $v'_x(x,t)$ are known functions of x and t; and h_o and Q_o are known functions of distance along the channel. In Eqs. 1–3, g is a known constant, q and v_x are known functions of x and t, while A, A_o, and R are measured properties of the channel cross-sectional geometry and are therefore known functions of x and the unknown h. The remaining parameter (n if the Manning equation is used to describe the friction slope, S_f, or C if the Chezy equation is used) is an empirical parameter that cannot be measured directly. For convenience, the Manning representation of the friction slope will be used throughout this paper without restricting the generality of the method presented herein. In natural river channels, the Manning n is a function of x and also a function of Q or h. When a numerical finite difference technique is used to solve the unsteady flow equations, the value of n is also a function of the particular schematization used to describe the continuous channel geometry by a series of discrete representations along the reach of channel being modeled.

The determination of n is the major task required in the calibration of one-dimensional unsteady flow models. An obvious and presently used method to determine n is by a trial-and-error technique in which the governing equations, Eqs. 1 and 2, are repeatedly solved by a finite difference technique for different assumed functions of $n(x, Q, \text{or } h)$. The particular functions that give the closest agreement between the solutions of the governing equations (subject to the particular boundary and initial conditions given by Eqs. 4–9) and the field observations are selected as the correct n function. Even when n is assumed to not vary with Q or h, the task can be extremely tedious, expensive, and difficult, since the governing equations are nonlinear. Also, when the channel reach is a part of a river system, the flow in a branch (tributary) can affect the flow both upstream and downstream in the main-stem river as well as the flow in other tributaries. This is particularly true of large rivers with major tributaries. When the bottom slope is very mild [in the range of 2 ft/mile (0.38 m/km) or less], an adjustment of n for one reach has repercussions upstream and downstream on the main stem and its tributaries.

The purpose of this paper is to present a simple and very efficient technique to determine the optimum n values as functions of x and h or Q when observed values of water surface elevation (stage) and discharge are available from

identification (calibration) technique presented in this paper, is related conceptually to an aquifer identification technique proposed in 1968 by Haines, Perrine, and Wismer (11). With this exception, the decomposition method has not been utilized; nevertheless, when applied to dendritic river systems, decomposition offers a means of greatly simplifying an otherwise complex mathematical problem and allowing the use of the simple optimization technique presented herein. River system decomposition is in no way restricted to use only with the Newton-Raphson solution technique. Other optimization techniques could be used with the principle of decomposition.

Theory

Basic Formulation.—Consider a reach of channel between two gaging stations where stage h'_A and discharge Q'_A are measured at the upstream station and stage h'_B only is measured at the downstream station as shown in Fig. 1. Eqs. 1 and 2, which describe the unsteady flow within the elementary reach, may be solved by a weighted four-point nonlinear implicit finite difference technique as described elsewhere by the first writer (6,7,8). This technique is similar to that used by Amein and Fang (1), Contractor and Wiggert (5), and others. The initial conditions of stages and discharges at all computational nodes along the reach A-B must be specified as well as the boundary conditions at the extremities of the reach. The upstream boundary condition is a known discharge hydrograph, i.e.

$$Q_A = Q'_A(t) \quad \ldots \quad (10)$$

and the downstream boundary condition is known stage hydrograph, i.e.

$$h_B = h'_B(t) \quad \ldots \quad (11)$$

Also, all lateral inflows or outflows denoted by Eqs. 8 and 9 must be known.

By specifying the known discharge hydrograph at the upstream boundary, any flow disturbances occurring upstream of the reach A-B that could affect the flow within reach A-B are taken into account. Likewise, by specifying the known stage at the downstream boundary, any disturbances occurring downstream of reach A-B such as backwater from tributary inflow or tidal effects that could influence the flow within reach A-B are effectively considered.

The n value is considered to be an integrated value throughout the reach A-B, i.e., n is not considered to vary with distance between the two gaging stations. However, n may vary with stage or discharge. In this paper, n will vary only with discharge and this variation can be described as a continuous piecewise linear function as shown in Fig. 2. The discharge is expressed as an average discharge throughout reach A-B. The total range of possible discharges is divided into a number ($j = 1, 2, 3, \ldots J$) of strata. Each stratum is associated with an $(n, \bar{Q})$ break-point in the $n(\bar{Q})$ piece-wise linear function.

From inspection of Eq. 3 it is apparent that n is a function of both Q and h; therefore, in order to determine a unique $n(\bar{Q})$ function for reach A-B, the discharge in the reach as well as the stage must be specified. The two boundary conditions given by Eqs. 10 and 11 provide the necessary combination of Q and h to allow a unique determination of n.

Optimization Algorithm.—In order to determine the appropriate $n(\bar{Q})$ function

for reach A-B, a trial $n(\bar{Q})$ function is selected and Eqs. 1 and 2 are solved subject to the specified boundary conditions, Eqs. 10 and 11. An optimal $n(\bar{Q})$ function is sought which will minimize the absolute value of the sum of the differences between the computed stages, h_A, and the measured stages, h'_A, at the upstream boundary.

The overall objective function chosen for minimization is

$$\min \phi_T = \left| \sum_{j=1}^{J} \phi_j \right| \quad \ldots \ldots \ldots \ldots \ldots \ldots \ldots \ldots \ldots \ldots \quad (12)$$

$$\text{in which} \quad \phi_j = \frac{1}{M_j} \sum_{i=1}^{M_j} h^i_A - h'^i_A \quad \ldots \ldots \ldots \ldots \ldots \ldots \ldots \ldots \quad (13)$$

in which M_j denotes the total number of stages associated with discharges within

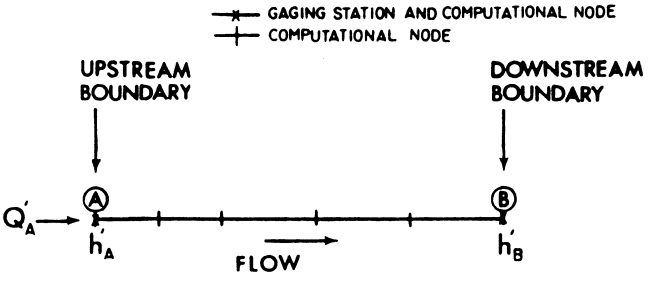

FIG. 1.—Schematic of Elementary Channel Reach A-B

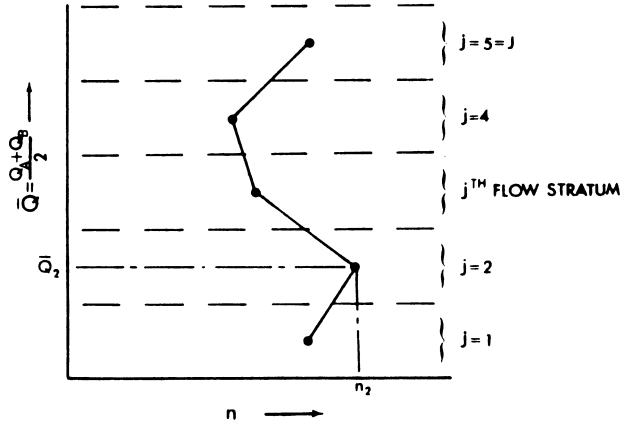

FIG. 2.—Typical $n(\bar{Q})$ Functional Relationship for Channel Reach A-B

the jth discharge stratum as shown in Fig. 2.

In order to determine the appropriate correction to each stratum of the $n(\bar{Q})$ function, it is desirable to work with an objective function for each stratum, i.e., ϕ_j as defined by Eq. 13. However, since

$$\left| \sum_{j=1}^{J} \phi_j \right| \leq \sum_{j=1}^{J} |\phi_j| \quad \ldots \ldots \ldots \ldots \ldots \ldots \ldots \ldots \ldots \ldots \quad (14)$$

the overall objective function, ϕ_T, will be minimized by minimizing each ϕ_j.

The objective function for the jth stratum, ϕ_j, may also be expressed in the following functional form:

$$\min \phi_j\{h_{A_j}[n_j(\bar{Q}_j)]\}; \quad j = 1, 2, \ldots J \quad \ldots\ldots\ldots\ldots\ldots\ldots \quad (15)$$

in which ϕ_j is a function of the computed and measured stages (h_A and h'_A) associated with discharges in the jth stratum as indicated in Eq. 13. The stages are also functions of the Manning n at the jth stratum, and the Manning n is a function of the average discharge $\bar{Q}_j$ within reach A-B.

An equivalent form of Eq. 15 is

$$\phi_j\{h_{A_j}[n_j(\bar{Q}_j)]\} = 0; \quad j = 1, 2, \ldots J \quad \ldots\ldots\ldots\ldots\ldots\ldots\ldots\ldots \quad (16)$$

By expressing Eqs. 13 or 15 in the form of Eq. 16, a gradient-type modified Newton-Raphson algorithm can be applied to determine the improved $n(\bar{Q})$ functions so as to minimize ϕ_j. The modification of the Newton-Raphson algorithm consists of the replacement of the continuous derivative with a finite difference derivative. Thus, upon applying the modified Newton-Raphson algorithm to Eq. 16, the following expression is obtained for determining the improved n_j trial value:

$$n_j^{k+1} = n_j^k - \frac{\phi_j^k(n_j^k - n_j^{k-1})}{\phi_j^k - \phi_j^{k-1}}; \quad k \geq 2; \quad j = 1, 2, \ldots J \quad \ldots\ldots\ldots\ldots \quad (17)$$

in which the kth superscript denotes the number of iterations. Eq. 17 can only be applied for the second and successive iterations because of the $k - 1$ terms in the numerical derivative portion of Eq. 17. Therefore, the first iteration is made using the following algorithm:

$$n_j^{k+1} = n_j^k \frac{1.00 - 0.01\,\phi_j^k}{|\phi_j^k|}; \quad k = 1; \quad j = 1, 2, \ldots J \quad \ldots\ldots\ldots\ldots \quad (18)$$

in which a small percentage change in n is made in the correct direction as determined by the term $(-\phi_j^k/|\phi_j^k|)$. The convergence properties of Eq. 17 are quadratic. Usually convergence is obtained within $3 \leq k \leq 5$ iterations. Convergence is obtained when either of the following inequalities is satisfied:

$$\phi_T^k = \frac{1}{J}\sum_{j=1}^{J} \phi_j^k < \epsilon \quad \ldots\ldots\ldots\ldots\ldots\ldots\ldots\ldots\ldots\ldots \quad (19)$$

$$\phi_T^k \geq \phi_T^{k-1} \quad \ldots\ldots\ldots\ldots\ldots\ldots\ldots\ldots\ldots\ldots\ldots\ldots \quad (20)$$

in which ϵ is a convergence criterion; an ϵ of 0.001 ft (0.0003 m) has been found to be a sufficiently small value.

The quality of the first trial (starting) values, n_j^1, for the $n(\bar{Q})$ function influences the required number of iterations. If the starting values deviate from the optimal values by too great a margin, Eq. 17 will not converge. This is easily remedied by assuming new starting values and repeating the procedure. Starting values may simply be judicious guesses or they may be estimated from the following application of the Manning equation:

$$n_j^1 = \frac{1}{M_j}\sum_{i=1}^{M_j} \frac{1.486\,AR^{2/3}\left(\dfrac{h'_{A_i} - h'_{B_i}}{x_A - x_B}\right)^{1/2}}{(Q'_A + q'\Delta x)_i} \quad \ldots\ldots\ldots\ldots\ldots\ldots \quad (21)$$

From the preceding theory, an optimization algorithm can be formulated for

determining the optimal $n(\bar{Q})$ function of an elementary reach; it consists of the following steps:

Step 1. Initial values of the $n(\bar{Q})$ function are made from Eq. 21 or are simply estimated.

Step 2. Eqs. 1 and 2 are solved by a finite difference technique subject to the boundary conditions, Eqs. 10 and 11, and the specified initial conditions and lateral inflows. The objective function, Eq. 12, is then determined for each stratum of discharges in the $n(\bar{Q})$ function using the computed and observed stages at the upstream boundary.

Step 3. Improved values of the $n(\bar{Q})$ function are obtained from Eq. 18 for the first iteration only and from Eq. 15 for the second and succeeding iterations.

Step 4. The objective function is evaluated and compared to see if it is less than a small specified ϵ value. If it satisfies either inequality, Eqs. 19 or 20, the optimal $n(\bar{Q})$ function has been determined; otherwise, return to step 2.

Decomposition of River System.—A river system consisting of either multiple reaches or multiple reaches and tributaries may be decomposed in such a way that the preceding optimization algorithm for an elementary reach may be applied reach-by-reach to the entire river system. The decomposition of a river system into elementary reaches for which optimal n values may be obtained reach-by-reach greatly simplifies the optimization problem and allows the calibration process to be accomplished in a most efficient manner.

First, consider the multiple-reach system shown in Fig. 3(*a*) with the gaging stations at points A, B, C, and D. Discharge is observed at A and stages are observed at A, B, C, and D. This multiple-reach system may be decomposed into three elementary reaches as shown in Fig. 3(*b*). The upstream reach A-B is treated first. Using the observed discharge, Q_A, and the observed stage, h_B, as the upstream and downstream boundaries, respectively, the unsteady flow equations are solved with a starting $n(\bar{Q})$ function either assumed or estimated from Eq. 21. The objective function that is to be minimized is the bias at point A, i.e., $\phi_A = h_A - h'_A$. Eqs. 17 and 18 are used to obtain improved values of n while simultaneously minimizing ϕ_A. As previously mentioned, any flow affecting reach A-B is accounted for by the upstream boundary condition, Q_A, while anything occurring downstream of point B which might affect the flow in A-B is taken into account by the downstream boundary condition of the observed stage h_B. Once the optimal $n(\bar{Q})$ function is obtained for reach A-B, the computed discharge, Q_B, is then used as the upstream boundary condition for reach B-C. In this way, the optimization process can proceed reach-by-reach in the downstream direction.

Next, consider the multiple-reach system with a tributary as shown in Fig. 4(*a*) with gaging stations at points A, B, C, and D. Discharge is observed at the upstream points on each river, i.e., at points A and D. This river system may be decomposed into three elementary reaches as shown in Fig. 4(*b*). First, the tributary reach is treated. The discharge at D is used as the upstream boundary condition for reach D-E. Since there is no gaging station at the confluence E, the stage at E is interpolated from observed stages at B and C. By using the interpolated stage, h_E, as the downstream boundary condition, any backwater

effects that the main-stem river has on the tributary are effectively considered. The unsteady flow equations with a starting $n(\bar{Q})$ function are then solved. Improved n values are obtained from Eqs. 17 and 18 so as to minimize the bias at D. The computed discharge at E coincident with the optimal $n(\bar{Q})$ function obtained from Eq. 18 is saved for use as lateral inflow q when optimizing reach B-C. Next, the multiple reach system (A-B and B-C) is treated, starting with the first upstream reach A-B. Then, when reach B-C is optimized, the effect of the tributary on the main stem is effectively considered by introducing as lateral inflow the tributary flow Q_E over the small Δx reach containing the confluence as shown in Fig. 4(*b*).

The decomposition principle can be used on a multiple-reach system with any number of tributaries. However, it is limited to river systems of dendritic

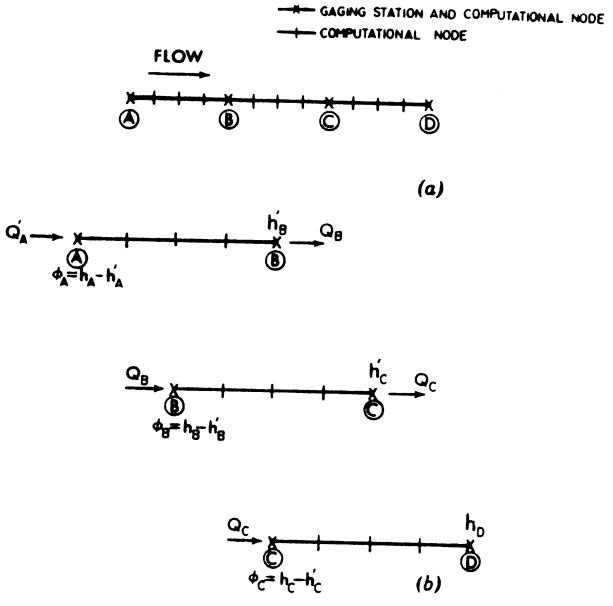

FIG. 3.—(*a*) Multiple-Reach River System; (*b*) Decomposed Multiple-Reach River System

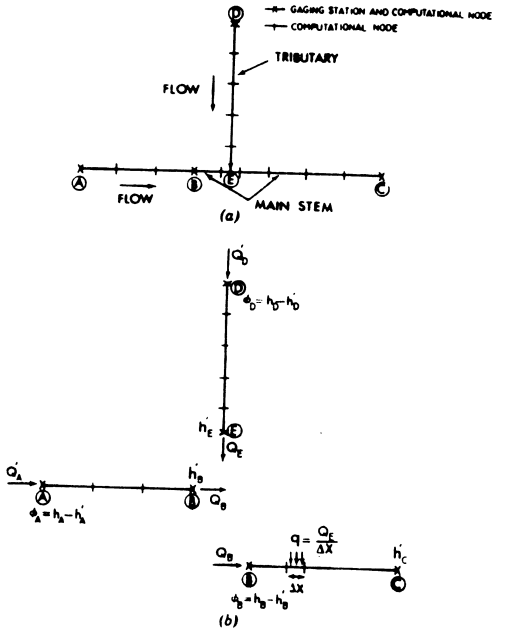

FIG. 4.—(*a*) Multiple-Reach River System with Tributary; (*b*) Decomposed Multiple-Reach River System with Tributary

configuration. An interconnecting system of channels is not amenable to the approach presented herein.

The basic formulation of the calibration procedure as described previously requires both discharge and stage observations. The observed discharges are required as an upstream boundary condition and the observed stages required as a downstream boundary condition. The objective function for determining the optimal $n(\bar{Q})$ function is composed of both computed and observed stages at the upstream boundary. For reasons of brevity, only this set of required observations is formulated herein; however, there are other possible combinations of observations. Another combination that the writers have also provided for in the computer coding of the calibration technique presented herein consists of the following: (1) Observed stage hydrograph for upstream boundary condition; (2) observed stage hydrograph for downstream boundary condition; and (3)

observed discharge hydrograph at downstream boundary for the objective function.

The writers have found that the first set of required observations (upstream stages-discharges and downstream stages) is well suited for most applications on large rivers where stage observations are much more plentiful than discharge observations. Actually, when multiple reaches are treated, only observed stages are required at all gaging points other than the most upstream station where observed discharges also are required.

Applications

Multiple-Reach Idealized Channel.—The essential features of the optimization algorithm are illustrated by identifying the $n(\bar{Q})$ functions for a multiple-reach

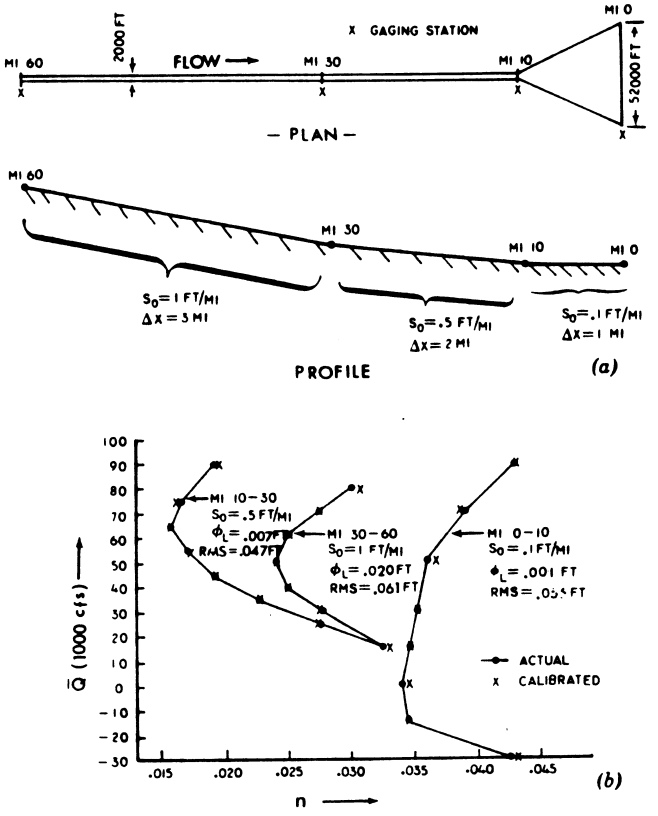

FIG. 5.—(*a*) Plan and Profile of Multiple-Reach Idealized Channel; (*b*) Actual and Calibrated $n(\bar{Q})$ Functions for Ideal Channel

idealized channel. The channel is 60 miles (97 km) long with a trapezoidal cross section having side slopes of 1:10 and a bottom width varying from 2,000 ft–52,000 ft (610 m–15,900 m) as shown in Fig. 5(*a*). The channel has a bed slope, S_o, which varies from 1.0 ft/mile (0.0001894) in the upstream reach to 0.1 ft/mile (0.019 m/km) in the downstream reach as shown in Fig. 5(*a*). The 60-mile (97-km) channel consists of three reaches, each bounded by gaging stations located at channel miles 60, 30, 10, and 0 (97 km, 48 km, 16 km, and 0 km). Lateral inflow is negligible and initial conditions are a steady flow of 20,000 cfs (560 m^3/s) and constant depth of 5.0 ft (1.5 m). At the upstream boundary

TABLE 1.—Comparison of Calibration Technique and DWOPER Forecast Program

Application (1)	Calibration Technique		Forecast Program (DWOPER)	
	Root-mean-square, in feet (meters) (2)	CPU time, in seconds (3)	Root-mean-square, in feet (meters) (4)	CPU time, in seconds (5)
Ideal	0.057 (0.017)	12.2	—	7.4
Multiple reach	0.31 (0.095)	21.4	0.44 (0.134)	10.9
Multiple-reach dendritic system	0.62 (0.189)	20.2	0.67 (0.204)	12.4

TABLE 2.—Summary of Results from All Runs of Idealized Channel Problem

Run (1)	Reach (2)	Iteration (3)	ϕ_T, in feet (meters) (4)	Root-mean-square, in feet (meters) (5)	CPU time, in seconds (6)	ϕ_T, in feet (meters) (7)	Root-mean-square, in feet (meters) (8)
1	1	0	−0.581 (−0.177)	0.757 (0.231)			
		1	−0.548 (−0.167)	0.721 (0.220)			
		2	−0.030 (−0.009)	0.143 (0.044)			
		3	0.015 (0.005)	0.073 (0.022)			
	2	0	0.683 (0.208)	1.444 (0.440)			
		1	0.655 (0.203)	1.399 (0.427)	17.0	−0.021 (−0.006)	0.153 (0.047)
		2	−0.140 (−0.043)	0.230 (0.070)			
		3	0.006 (0.002)	0.116 (0.035)			
	3	0	−1.244 (−0.379)	1.390 (0.424)			
		1	−1.221 (−0.372)	1.365 (0.416)			
		2	−0.213 (−0.065)	0.331 (0.101)			
		3	0.083 (0.025)	0.271 (0.083)			
2	1	0	0.015 (0.005)	0.073 (0.022)			

TABLE 2.—*Continued*

(1)	(2)	(3)	(4)	(5)	(6)	(7)	(8)
		1	0.014	0.058			
			(0.004)	(0.018)			
		2	−0.007	0.047			
			(−0.002)	(0.014)			
	2	0	0.038	0.085			
			(0.012)	(0.026)			
		1	0.038	0.070	12.2	−0.009	0.057
			(0.012)	(0.021)		(−0.003)	(0.017)
		2	−0.075	0.134			
			(−0.023)	(0.041)			
		3	−0.020	0.061			
			(−0.006)	(0.019)			
	3	0	0.001	0.056			
			(0.000)	(0.017)			
3	1	0	0.495	0.668			
			(0.151)	(0.204)			
		1	0.448	0.630			
			(0.137)	(0.192)			
		2	−0.006	0.108			
			(−0.002)	(0.033)			
		3	−0.031	0.081			
			(−0.009)	(0.025)			
	2	0	−0.988	1.249			
			(−0.301)	(0.381)			
		1	−0.974	1.225	14.1	−0.005	0.092
			(−0.297)	(0.374)		(−0.002)	(0.028)
		2	0.932	0.233			
			(0.284)	(0.071)			
		3	0.010	0.114			
			(0.003)	(0.035)			
	3	0	−0.159	0.336			
			(−0.048)	(0.102)			
		1	−0.147	0.313			
			(−0.045)	(0.095)			
		2	0.006	0.080			
			(0.002)	(0.024)			

Note: Starting values of $n(\bar{Q})$ for Run 1 are constant n values of 0.025 for each reach. Starting values of $n(\bar{Q})$ for Run 2 are smoothed n values from Run 1. Starting values of $n(\bar{Q})$ for Run 3 are constant n values of 0.032, 0.017, and 0.037.

The channel is subjected to a typical single-peaked discharge hydrograph that has a peak flow of 100,000 cfs (2,800 m^3/s) occurring at $t = 31$ hr and receding to the initial steady flow rate at $t = 81$ hr. The downstream boundary is a sinusoidal stage hydrograph of 5.0 ft (1.5 m) amplitude and 24-hr period.

The actual $n(\bar{Q})$ functions for each of the three reaches are shown in Fig. 5(*b*). Stage observations at the gaging stations [channel miles 60, 30, and 20 (97 km, 48 km, and 32 km)] were simulated by obtaining a numerical solution of Eqs. 1 and 2 subject to the initial and boundary conditions, channel geometry,

and $n(\bar{Q})$ functions described previously. The four-point implicit method me tioned previously was used in the National Weather Service's Operatio Dynamic Wave Forecast Program (DWOPER) to integrate the unsteady fl equations using time steps of 1 hr and distance steps as indicated in Fig. 5(The simulated stages and discharges serve as a set of true observations, i. the data are free of observer noise (any noise originating from the numeri solutions is duplicated in the calibration procedure). Also, the geometri properties of the idealized channel are exactly identifiable, i.e., observatio and sampling errors are absent.

Next, the simulated stages at the gaging stations [channel miles 60, 30, a 20 (97 km, 48 km, and 32 km)] along with the discharge and stage bound conditions were used as input for the optimization algorithm to uncover actual $n(\bar{Q})$ functions. In run No. 1, constant $n(\bar{Q})$ functions of 0.025 we used as starting values for each of the three reaches. The optimization algorit consisting of the four steps previously outlined was applied sequentially to upstream, middle, and downstream reaches. The final ϕ_T values for all discha strata were 0.015 ft (0.004 m), 0.006 ft (0.002 m), and −0.083 ft (−0.025 for each of the three reaches. The final root-mean-square errors between observed and computed stages at the upstream station in each of the th reaches were 0.073 ft (0.022 m), 0.116 ft (0.035 m), and 0.271 ft (0.083 Three iterations were required for each reach. Computer time (IBM 360/1 required by the optimization algorithm was 12.2 sec; this is approximately times that required for simulating the observations using the National Weat Service's DWOPER forecast program as indicated in Table 1.

The optimal $n(\bar{Q})$ function is dependent on the starting values. This is illustra by three separate runs made with different starting values as summarized Table 2. Run 2, in which starting values were obtained by smoothing the opti values from run 1, shows improved statistics, with the average rms error be reduced 0.153 ft (0.047 m) in run 1 to a value of 0.057 ft (0.017 m). The opti $n(\bar{Q})$ function obtained from run 2 is shown in Fig. 5(*b*) along with the ac $n(\bar{Q})$ function used to generate the observations. This illustrates the poten ability of the calibration technique consisting of the optimization algorithm system decomposition principle to uncover the actual $n(\bar{Q})$ functions. computed and observed stages at channel mile 10 (16 km) using the opti $n(\bar{Q})$ function [miles 0–10 (0 km–16 km)] are shown in Fig. 6. The stag this gaging station is significantly affected by the sinusoidal stage fluctua at channel mile 0.

Multiple-Reach River.—Currently, the calibration technique is being used the National Weather Service to develop forecast procedures for a num of major rivers throughout the nation. Included among these is the Mississ River commencing at Vicksburg and terminating 460 miles (741 km) downstr at the Gulf of Mexico, as shown in Fig. 7. Along this reach, the low f depth varies from approx 25 ft (7.6 m) at some crossings to a maximum b depth of almost 200 ft (61 m). The width is variable with an average of a 1/2 mile (0.8 km). The bottom slope is variable. The upper 100 miles km) has an average effective hydraulic slope of 0.320 ft/mile (0.061 m/k the middle 125 miles (201 km) has an average effective slope of 0.076 ft/ (0.014 m/km), and the lower 225 miles (362 km) has an average effective s of 0.002 ft/mile (0.0004 m/km). Discharge varies from approx 150,000

2,000,000 cfs (420 m^3/s–56,000 m^3/s). Approximately 25% of the flow is diverted through the Old River Diversion structure into the Atchafalaya Floodway. The diversion structures at Morganza and Bonnet Carre as shown in Fig. 7 operate only during extremely large flood events. The 460-mile (740-km) reach consists

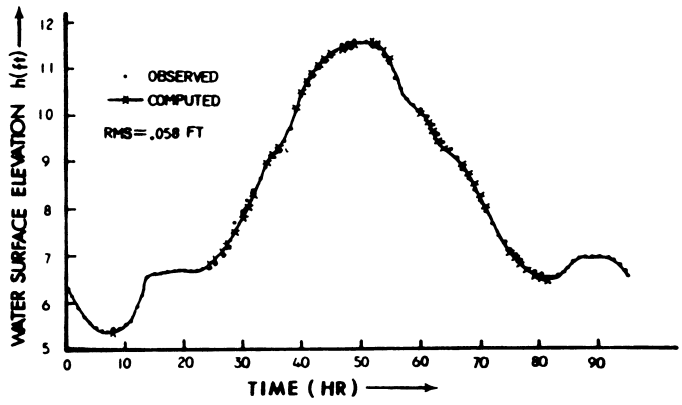

FIG. 6.—Computed and Observed Stages for Mile 10 of Idealized Channel

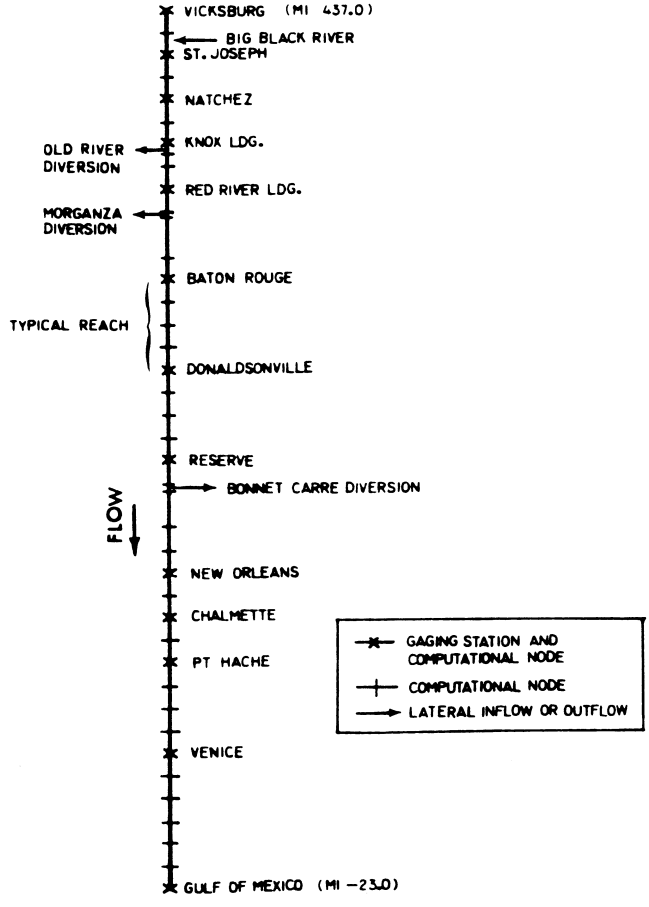

FIG. 7.—Schematic of Lower Mississippi Multiple-Reach System

of 12 multiple reaches, each bounded by gaging stations as shown in Fig. 7.

The calibration technique was applied to this multiple reach to determine the $n(\bar{Q})$ function for each reach for much of the 1973 flood. The duration of the hydrograph was 91 days. Time steps of 24 hr and variable distance

steps averaging about 10 miles (16 km) were used in the four-point impl solution step of the optimization algorithm. Starting values for the $n(\bar{Q})$ functio were obtained from Eq. 21. The 1973 flood input consisted of observed discha hydrographs at Vicksburg and at the three diversion structures that opera during this extreme event, and the lateral inflow from the Big Black Riv Observed stage hydrographs at the 13 gaging stations shown in Fig. 7 w also used as input. The average ϕ_T value for all 12 reaches was 0.001 ft (0.0 m) and the average root-mean-square was 0.31 ft (0.095 m). A typical exam of the optimal computed and observed stage hydrograph is presented in F 8(*a*) for the Baton Rouge gaging station. The final $n(\bar{Q})$ function for the Bat Rouge-Donaldsonville reach is shown in Fig. 8(*b*). The n values are wit

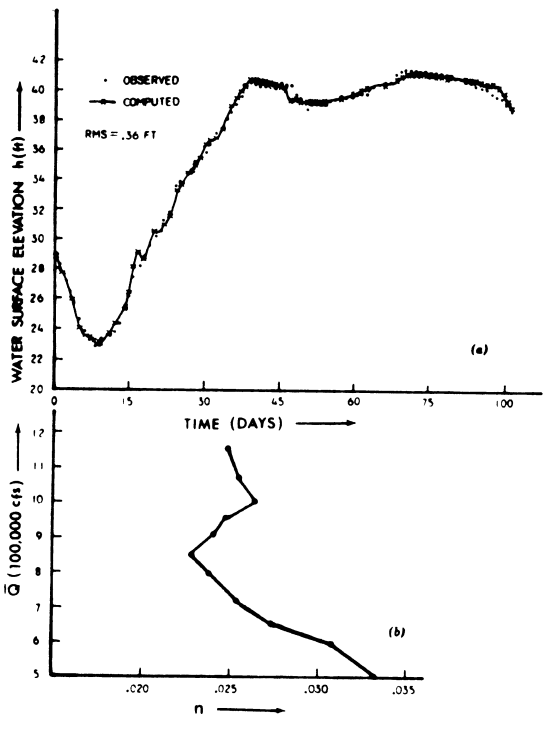

FIG. 8.—(*a*) Computed and Observed Stages for Baton Rouge of Lower Mississippi System; (*b*) Optimal $n(\bar{Q})$ Function for Baton Rouge-Donaldsonville Reach of Lower Mississippi System

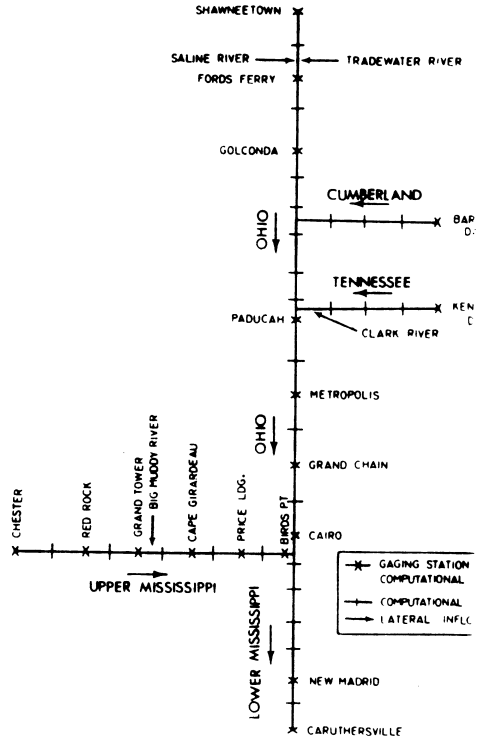

FIG. 9.—Schematic of Mississippi-Oh Cumberland-Tennessee (MOCT) Syst

the range of values computed using steady-state techniques. The trend show n to decrease with increasing discharge is reasonable for this reach as it a large river having levees on both sides with a very small overbank area relati to the channel flow-area.

Note that the root-mean-square value does not approach zero as closely this application as in the preceding example of the idealized channel even thou the ϕ_T value does vanish. The tendency for ϕ_T to approach zero more read than the root-mean-square value can be observed in the idealized problem althou there the deviation of the root-mean-square value from zero is insignifica The inability of the optimization algorithm to drive the root-mean-square va to nearly zero as ϕ_T is reduced to essentially zero is considered to be d

to the presence of noise (errors) in the observed stages, discharges, and cross-sectional properties. Nonetheless, a root-mean-square value of 0.31 ft (0.095 m) is considered to be quite within the limits of practical accuracy.

An average of three iterations was required for each reach, and the total required computation time for all 12 reaches was 21.4 sec, as shown in Table 1. This compares with 10.9 sec required for reconstituting the observed stages using the optimal $n(\bar{Q})$ functions in the DWOPER program.

Multiple-Reach Dendritic River System.—The calibration technique has also been used to determine the optimal $n(\bar{Q})$ functions for the Mississippi-Ohio-Cumberland-Tennessee (MOCT) River system, shown in Fig. 9. This 393-mile (633-km) river system consists of 15 multiple reaches bounded by the gaging stations as shown in Fig. 9. The system is dendritic configuration with observed discharges available at the upstream gaging stations on each of the four rivers (Shawneetown on the Ohio, Barkley Dam on the Cumberland, Kentucky Dam on the Tennessee, and Chester on the upper Mississippi). Stage observations are available at all gaging stations. The main-stem river is considered for mathematical modeling purposes to be the Ohio-lower Mississippi segment with the upper Mississippi,

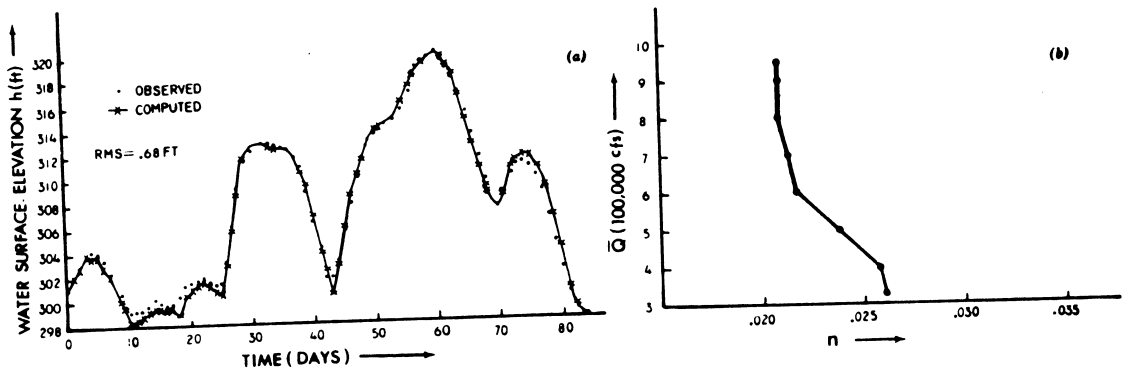

FIG. 10.—(*a*) Computed and Observed Stages for Cairo of MOCT System; (*b*) Optimal $n(\bar{Q})$ Function for Cairo-New Madrid Reach of MOCT System

Cumberland, Tennessee Rivers considered as tributaries. The bed slope is variable with an average effective hydraulic slope of about 0.25 ft/mile (0.047 m/km) to 0.50 ft/mile (0.095 m/km). Each branch of the river system is subject to backwater effects due to flows in the other branches. Total discharge through the system varies from approx 120,000 cfs–1,700,000 cfs (3,400 m^3/s–47,600 m^3/s).

As a final illustration, the calibration technique was applied to the MOCT system for the 1970 flood event of 83 days duration. Time steps of 24 hr and variable distance steps averaging approx 9 miles (15 km) were used in the implicit four-point solution of Eqs. 1 and 2. The river system was decomposed such that the $n(\bar{Q})$ function was optimized for each of the individual tributaries. Then, the multiple-reach main stem from Shawneetown to Caruthersville was optimized using the computed downstream discharges from the previously optimized tributaries as lateral inflows. The average ϕ_T value for all 15 reaches was 0.048 ft (0.015 m), and the average root-mean-square error was 0.62 ft (0.20 m). A typical example of the optimal computed and observed stage

hydrograph is presented in Fig. 10(*a*) for the Cairo gaging station. The opti $n(\bar{Q})$ function for the Cairo-New Madrid reach is shown in Fig. 10(*b*). average of three iterations was required for each reach and the total computat time for all 15 reaches was 20.2 sec as shown in Table 1. The somewhat lar root-mean-square value for the MOCT system as compared with the previ Lower Mississippi application is considered to be due to the greater temp variation of the flows in the MOCT system. If $n(\bar{Q})$ functions for each re were selected as the average n for the discharge range, i.e., $n(\bar{Q})$ = consta the average root-mean-square error for all 15 reaches in a simulation run DWOPER was 1.32 ft (0.403 m). This compares with the value of 0.67 ft (0 m) if the calibrated $n(\bar{Q})$ functions were used in a DWOPER run as sho in Table 1. The substantial increase indicates the significance of the n relationship.

Summary and Conclusions

A technique is presented for determining the optimal $n(\bar{Q})$ function for reach of river bounded by gaging stations. The technique uses a gradient-ty modified Newton-Raphson algorithm to improve the initial trial $n(\bar{Q})$ functi such that the difference between upstream observed and computed stages minimized. The computed stages are obtained from a four-point implicit fin difference solution of the one-dimensional unsteady flow equations subject upstream and downstream boundary conditions of observed discharge and sta hydrographs, respectively. The technique is not restricted to this particular fin difference solution. The technique may be applied to a river system consisti of multiple reaches or tributaries, or both, forming a dendritic configurati by utilizing the principle of system decomposition. When river systems a treated, discharge observations are required only at the upstream extremit of the main stem and each tributary while stages are required at all gagi stations. This requirement is well suited to large, flat rivers where backwa complicates discharge observations.

The technique is simple in concept and very efficient computationally sin the optimization algorithm converges quadratically with usually only three four iterations required. An ideal channel system subjected to complex unstea flow hydraulics and Manning n-discharge functions is used to illustrate t technique's ability to uncover the actual $n(\bar{Q})$ function when observational erro are absent. The technique has been applied by the National Weather Servi to several natural river systems; partial summaries of two of such applicatio were presented to illustrate the efficiency and ability of the calibration techniq to determine the optimal $n(\bar{Q})$ functions for river systems having complicat unsteady flow hydraulics and imperfect observations. The observed-comput stage hydrograph root-mean-square error coincident with the optimal $n(\bar{Q})$ function ranges from 0.2 ft–0.7 ft (0.06 m–0.21 m). The required computati time (IBM 360/195) is about 0.005 sec/$\Delta x/\Delta t$. Using the DWOPER foreca program and optimal $n(\bar{Q})$ functions from the calibration technique, the simulati of a total river system produces average root-mean-square errors (see Tab 1) that show little deterioration from the average of the root-mean-square valu of the decomposed elementary reaches as treated in the calibration technique.

APPENDIX.—REFERENCES

1. Amein, M., and Fang, C. S., "Implicit Flood Routing in Natural Channels," *Journal of the Hydraulics Division*, ASCE, Vol. 96, No. HY12, Proc. Paper 7773, Dec., 1970, pp. 2481–2500.
2. Becker, L., and Yeh, W. W.-G., "Identification of Parameters in Unsteady Open Channel Flows," *Water Resources Research*, Vol. 8, No. 4, Aug., 1972, pp. 956–965.
3. Becker, L., and Yeh, W. W.-G., "Identification of Multiple Reach Channel Parameters," *Water Resources Research*, Vol. 9, No. 2, Apr., 1973, pp. 326–335.
4. Bennett, J. P., "General Model to Simulate Flow in Branched Estuaries," *Proceedings of the Symposium on Modeling Techniques*, Waterways, Harbors and Coastal Engineering Division, ASCE, Sept., 1975, pp. 643–662.
5. Contractor, D. N., and Wiggert, J. M., "Numerical Studies of Unsteady Flow in the James River," *VPI-WRC-BULLETIN 51*, Water Resources Research Center, Virginia Polytechnic Institute and State University, Blacksburg, Va., May, 1972, 56 pp.
6. Fread, D. L., "Effect of Time Step Size in Implicit Dynamic Routing," *Water Resources Bulletin*, American Water Resources Association, Vol. 9, No. 2, Mar., 1973, pp. 338–351.
7. Fread, D. L., "Numerical Properties of Implicit Four-Point Finite Difference Equations of Unsteady Flow," *NOAA Technical Memorandum NWS HYDRO-18*, U.S. Department of Commerce, National Oceanic and Atmospheric Administration, National Weather Service, Washington, D.C., Mar., 1974.
8. Fread, D. L., "Flood Routing in Meandering Rivers with Flood Plains," *Proceedings of the Symposium on Inland Waterways for Navigation, Flood Control, and Water Diversions*, Waterways, Harbors and Coastal Engineering Division, ASCE, Aug., 1976, pp. 16–35.
9. Frind, E. O., and Pinder, G. F., "Galerkin Solution of the Inverse Problem for Aquifer Transmissivity," *Water Resources Research*, Vol. 9, No. 5, Oct., 1973, pp. 1397–1410.
10. Garay, H. L., Haimes, Y. Y., and Das, P., "Distributed Parameter Identification of Ground Water Systems by Nonlinear Estimation," *Journal of Hydrology*, Vol. 30, No. 1/2, May, 1976, pp. 47–61.
11. Haimes, Y. Y., Perrine, R. L., and Wismer, D. A., "Identification of Aquifer Parameters by Decomposition and Multilevel Optimization," *Contribution No. 123*, Water Resources Center, University of California, Los Angeles, Calif., Mar., 1968.
12. Kleinecke, D., "Use of Linear Programming for Estimating Geohydrologic Parameters of Groundwater Basins," *Water Resources Research*, Vol. 7, No. 2, Apr., 1971, pp. 367–374.
13. Lin, A. C., and Yeh, W. W.-G., "Identification of Parameters in an Inhomogeneous Aquifer by Use of the Maximum Principle of Optimal Control and Quasi-Linearization," *Water Resources Research*, Vol. 10, No. 4, Aug., 1974, pp. 829–838.
14. Marino, M. A., and Yeh, W. W.-G., "Identification of Parameters in Finite Leaky Aquifer System," *Journal of the Hydraulics Division*, ASCE, Vol. 99, No. HY2, Proc. Paper 9567, Feb., 1973, pp. 319–336.
15. Neuman, S. P., "Calibration of Distributed Parameter Groundwater Flow Models Viewed as a Multiple-Objective Decision Process under Uncertainty," *Water Resources Research*, Vol. 9, No. 4, Aug., 1973, pp. 1006–1021.
16. Rao, V. S., Contractor, D. N., and Tiyamani, C., "Optimal River Cross Sections for Flood Routing," *Proceedings of the Symposium on Inland Waterways for Navigation, Flood Control, and Water Diversions*, Waterways, Harbors and Coastal Engineering Division, ASCE, Aug., 1976, pp. 421–433.
17. Yeh, W. W.-G., and Becker, L., "Linear Programming and Channel Flow Identification," *Journal of the Hydraulics Division*, ASCE, Vol. 99, No. HY11, Proc. Paper 10177, Nov., 1973, pp. 2013–2021.
18. Yeh, W. W.-G., and Tauxe, G. W., "Quasilinearization and the Identification of Aquifer Parameters," *Water Resources Research*, Vol. 7, No. 2, Apr., 1971, pp. 375–381.
19. Yeh, W. W.-G., and Tauxe, G. W., "Optimal Identification of Aquifer Diffusivity

Using Quasilinearization," *Water Resources Research*, Vol. 7, No. 4, Aug., 1971 pp. 955–962.